Available online at www.sciencedirect.com
SCIENCE DIRECT
Polymer 46 (2005) 7191–7200
polymer
www.elsevier.com/locate/polymer

Charge consequences in electrospun polyacrylonitrile (PAN) nanofibers

Veli E. Kalayci, Prabir K. Patra*, Yong K. Kim, Samuel C. Ugbolue, Steven B. Warner*

Department of Textile Sciences, College of Engineering, University of Massachusetts Dartmouth, 285 Old Westport Road, North Dartmouth, MA 02747, USA

Received 3 March 2005; received in revised form 13 June 2005; accepted 15 June 2005
Available online 14 July 2005

Abstract

During the last 10 years extensive research has been conducted on various aspects of electrospinning. These efforts include spinning many different polymer and solvent pairs, varying fiber forming conditions, fiber characterization and process modeling. In this work we explore some issues related to charging of the polymer solution, namely charge quantification of electrospun fibers and different charge delivery designs. PAN fibers electrospun in our laboratory show a charge density of 30–50 nC/mg. The charge density varied with applied voltage and solution properties. Theoretical charge density calculations agree well with experimental measurements. Different charging approaches, such as positive or negative induction charging and ionized field charging, all led to fine fiber formation.

Keywords: Polymer materials; Electrospinning; Charged nanofibers

1. Introduction

Electrospinning is a technology that has been known at least since, the 1930's; however, it has not gained significant industrial importance largely because of the low output of the process, inconsistent and low molecular orientation, poor mechanical properties and high diameter distribution of the electrospun fibers. Donaldson Inc., a leading company that has been electrospinning for more than two decades produces only about 3 lbs. of electrospun fibers per day, which suggests that productivity of solution electrospinning is low. While solution electrospinning can be scaled up in obvious ways, efficient and clever scale up has thus, far remained elusive. Recently Lim et al. have reported the mechanical properties of a single polycaprolctone electrospun ultrafine fibers and the tested fiber exhibited characteristic low strength and low modulus but high extensibility at room temperature which is consistent with our [1] and others [2] rather crude measurements. Their results showed that mechanical properties were dependent on fiber diameter and the fibers with smaller diameter had higher strength but lower ductility presumable due to their greater attenuation during electrospinning. Although special needs of military, medical and filtration applications [3,4] have stimulated recent studies and renewed interest in the process, quantitative scientific information regarding the process is limited. The main advantages of the top–down electrospinning process are its relatively low cost compared to other bottom up methods, the resulting nanofibers are continuous and do not need expensive purification, unlike submicrometer-diameter whiskers, inorganic nanorods, carbon nanotubes and nanowires [5].

Traditional methods of polymer fiber production include melt spinning and solution spinning. These methods rely on mechanical forces to produce fibers—extruding polymer melt or solution through a spinneret and subsequently drawing the resulting filaments as they solidify or coagulate. Typical fiber diameters that result from these methods are in the range of 5–500 μm. In bi-component spinning designed to produce nanofibers, two incompatible materials, at least one being polymeric, are extruded together to form one filament using a special spinneret. The filament is then processed through the usual steps: Drawing, heat setting, and winding. The continuous phase is then removed, usually by dissolving, leaving behind as many as 1000 nanofibers [6]. Minimum fiber diameter that can be routinely produced is on the order of about a hundred nanometers. Meltblowing can also be used to make fibers down to about 1 μm in diameter [7], and split or bi-component melt blown fibers can be even smaller [8].

* Corresponding authors. Tel.: +1 508 999 8439; fax: +1 508 999 9139.
E-mail address: ppatra@umassd.edu (P.K. Patra).

0032-3861/$ - see front matter © 2005 Elsevier Ltd. All rights reserved.
doi:10.1016/j.polymer.2005.06.041

Electrospinning, a simple process to set up, requires a nominal electric field on the order of 1 kV/cm. In the process a polymer solution or melt is held by its surface tension at the end of a capillary, such as a stainless steel needle or a Pyrex or polyolefin pipette. As the intensity of the electric field is increased, usually by increasing the voltage, the hemispherical surface of the solution at the tip of the capillary tube elongates to form a structure known as a Taylor cone [9]. Mutual charge repulsion causes electrical forces to try to overcome the surface tension. At a certain voltage the electrical forces overcome the surface tension and a jet ejects from the Taylor cone. The jet travels some distance and then a whipping instability begins to further attenuate the jet into nanosize fibers. The fibers are collected onto a counter electrode, such as a screen, drum, plate, or the edge of a rotating disk. Coupled with the usual observations the fact that fibers can be electrospun using an Ac field indicates that a portion of the attenuation occurs in the stable jet region. That Dc electrospun fibers are smaller than Ac spun fibers indicates further drawing occurs in the instability region.

Using electrical forces alone, the electrospinning process can produce fibers with nanometer diameters. Because of their small diameters, electrospun fibers have a large surface-to-volume ratio, which enables webs of nanofibers to tenaciously absorb a wetting liquid. Small pores, defined by the spaces among electrospun fibers, are capable of capturing micron-sized particles which few of any other techniques can boast, and make electrospun webs suitable candidates for military and civilian filtration applications, as well as potential scaffolds for tissue growth [10]. Also, there is the option of incorporating additives into the fibers, making them potential drug delivery systems, antibacterial agents or super-paramagnetic field-responsive materials [11,12]. In addition, small diameter fibers have a low bending modulus, which manifests as a soft fabric hand.

2. Experimental

Our electrospinning apparatus consisted of a syringe pump, a 0–50 kV Dc power supply, an ammeter and various take up devices including metal screens, belts and other targets in an enclosed Faraday cage, as shown in the cartoon in Fig. 1.

We used polyacrylonitrile (PAN) in dimethylformamide for charge measurement work. The properties of the solutions are given in Table 1. Viscosity measurements were performed using a Brookfield DV-II+ programmable viscometer; electrical conductivity was measured with a Corning CD-55 conductivity meter; and surface tension was calculated using a combination of contact angle and capillary rise methods. The contact angle was measured using a Nrl-Ca goniometer when a glass capillary was immersed into a polymer solution.

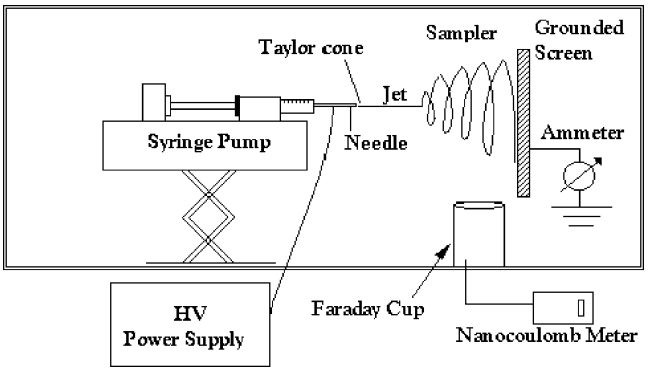

Fig. 1. Schematic of electrospinning and charge measurement set-up.

The charge on the web was measured using a nanocoulomb meter connected to a Faraday cup, as shown in Fig. 1. The fibers were spun onto a square of polyethylene film that we call a sampler and electrospun fibers were transferred to the Faraday cup immediately after spinning. The amount of charge on the substrate was determined. Then the sampler with its load was weighed using a Mettler-Toledo AG135 analytical balance. The weight of the clean target was subtracted. In this way, we measured the charge per mass of electrospun PAN fibers as a function of collection time, voltage and solution concentration. In order to understand the effect of solvent evaporation on current flow from the grounded electrode, we electrosprayed pure solvent and measured the current.

While induction charging using a negative charge is known in electrospinning, experimental studies are limited. When positive charging is used, the charges species are positive ions; however, in negative charging, the charges species are likely electrons. Since, electrons have much greater mobility than positive ions in an imperfect insulator, diffusion from the center of a fiber to the surface is much more rapid for electrons than ions. We were seeking to ascertain whether fibers spun using a negative charge differed from fibers made using a positive charge. We employed a negative charging unit that is ordinarily used for

Table 1
Polyacrylonitrile/DMF solution properties

	Viscosity (cP)	Temperature[a] (°C)	Conductivity (μS)	Surface tension (mN/m)	Solution compostion	
					Polymer	DMF
PAN-8	333.3	20.8	39.0	72.9	8.0	92.0
PAN-13	2800.0	21.4	50.0	97.6	13.0	87.0

[a] Temperature of the polymer solution during the viscosity measurement.

flocking. It has an output voltage of 40–70 kV and a power capacity of 15 W. The positive charging device was purchased from Gamma High Voltage Research, model E-50P. It has a voltage capacity of 0–50 kV and a power capacity of 20 W. Electrospinning was achieved once with a voltage of +40 kV and once with a voltage of −40 kV.

Our chief goal was to understand all sources of charging in electrospinning. To ascertain the effect of free ions created by dielectric breakdown of air, we adapted an ionized field charging technique that was originally used for crop spraying systems [13]. We disabled the wiring for directly inducing charge into the system and instead placed the syringe–needle system through an O-ring electrode, which was stressed at 30 kV, as shown in Fig. 2. The polymer solution used in these experiments was 8 wt% PAN/DMF. The polymer solution feed rate was 0.01 ml/min.

Electrospun fibers were viewed using a JEOL-JSM 5610 scanning electron microscope. To measure the fibers' diameter in a sample, a line was drawn on a photomicrograph and the diameter of the fibers was measured as close as practical to the cutting line. The results were then compiled into classes in order to obtain fiber diameter distribution profiles.

3. Results and discussion

3.1. Polymer solution properties

Various solution properties are given in Table 1. The two PAN solutions had 8 and 13 wt% polymer and their viscosities, conductivities and surface tensions differed.

3.2. Corona discharge

In the electrospinning process most of solvent evaporates while the jet and the nanofibers are moving to the grounded electrode. The solvent evaporates and forms a mist during continuous spinning. One of the several reasons for electrical discharge of the stored charge through the atmosphere surrounding the fibers may be the dielectric breakdown of the solvent. Corona parameters such as breakdown voltage and corona current depend on the dielectric properties of the gas medium, notably permittivity. Molecular structure and processes such as molecular excitation, ionization and the specifics of charge carrier interactions have an impact on charge transfer from one ionized molecule to another, which can be expressed in terms of the conduction of the gas surrounding the charged fibers.

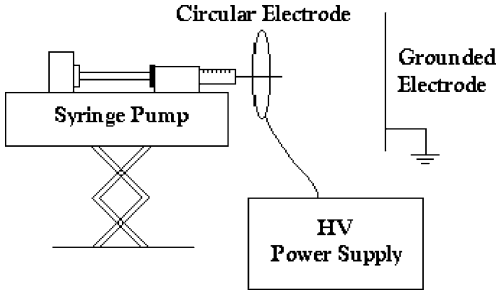

Fig. 2. Schematic of ionized field charging.

Electrospraying is better understood than is electrospinning, and much can be learned by analyzing electrospraying. Gaskell [14] divides the electrospraying process into three stages: Droplet formation, droplet shrinkage and gaseous ion formation. The solution delivered to the tip of the needle experiences the electric field associated with the maintenance of the tip at high potential. Using a positive potential results in accumulation of positive ions in the solution, which is thus, drawn out to establish a Taylor cone. At a sufficiently high-imposed field, the cone is drawn to a jet, which produces positively charged droplets when the applied electrostatic force exceeds the surface tension. Evaporation of solvent from the initially formed droplets leads to a reduction in diameter. Coulombic explosion occurs at the Rayleigh limit, the point at which the magnitude of the charge density is sufficient to overcome the surface tension holding a droplet together. Continuous depletion of the droplet size by solvent evaporation and Coulombic explosion, respectively, may be envisaged to result in principle eventually in the formation of droplets containing a single ion.

As explained using quantum chemical concept [15] solvent evaporation does not remove charge from the system in electrospraying or electrospinning; charged droplets evaporate losing mass without losing charge. Electrospinning is fundamentally similar to electrospraying, the key differences being that chain entanglements yield fibers rather than droplets and the forces required for Rayleigh bursting now include mechanical elements and are thus, commensurately higher. Tepper and co-workers demonstrated the use of Ac and Dc potential in the electrospraying of carboxymethylcellulose (CMC) onto semiconducting and insulating substrates. They showed that on semiconducting surface both Ac and Dc methods are capable of producing significant CMC coverage while Ac potential was capable of producing significant coverage only on the insulating substrate. According to them this may be because of possible reduction of surface charging. In comparison the electrospinning of PEO fibers using both Ac and Dc potential the Ac potential resulted in significant reduction in the amount of fiber whipping and higher degree of fiber alignment in the electrospun mats [16].

The results of discharge current measurements made using different solvents are given in Fig. 3. Perhaps the most interesting results were obtained using only solvent, which means the process was actually solvent electrospraying. The measurements were conducted without intentionally removing air from the spraying area. The solvent was placed in a syringe and charged positively as it traveled at a set rate to a

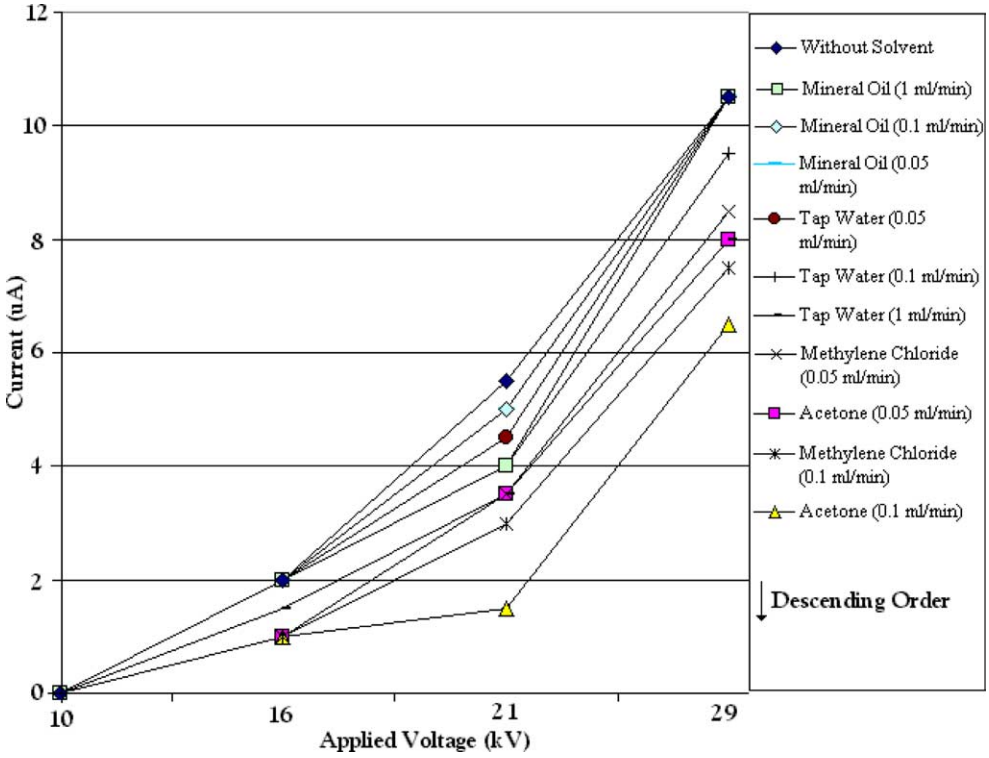

Fig. 3. Effect of solvent on current flow from the grounded electrode.

hole in the tip of a stainless-steel needle. This experiment was done in an enclosed polycarbonate box. The highest current flow from the collector to ground was achieved in the absence of any solvent. This current was formed by the ionization of the air at the needle tip at a sufficiently high electric field and causes the subsequent acceleration of the charges to the collector. Many different positive species were likely formed, but the most common dominant species created during electrical breakdown of unconditioned air is usually $H_3O^+(H_2O)_n$ [17].

All sprayed media were characterized in terms of their voltage–current characteristics, which have a typical parabolic shape, and are in good agreement with the corona voltage–current characteristic of some gases [18]. The current measured in experiments using tap water was higher than the current measured when methylene chloride was used. The current measured for methylene chloride was in turn higher than that measured when acetone was used. This result seems to be a consequence of the gas conduction of the plasma formed by the solvent evaporation, and gas conduction specifically depends on the permittivity of solvent molecules in the gaseous state. Allen et al. [19] reported that the breakdown voltages depend on the amount of water vapors in the air, which of course changes the permittivity of space. Hence, the breakdown voltage of the gap increases with increasing humidity. Insulative gases like sulfur hexafluoride can be used to increase the breakdown voltage and, therefore, reduce the magnitude of corona currents, but we did not pursue this avenue. Similarly, removing the sharp needle would reduce the field strength, but electrospinning might cease. Some researchers use two plates in their electrospinning apparatus, which would minimize corona formation, and perhaps eliminate it entirely.

The measured conductivity of the (liquid) solvents used is given in Table 2. The conductivity impacts the rate that charge can move within the solvent. Hence, it will affect electrospraying and perhaps electrospinning, from Taylor cone formation to discharge at the collector.

Another perhaps unexpected observation based on Fig. 3 is that the current flow decreased with increasing feed rate. For a given period of time higher feed rate results in a higher amount of solvent mist that can interact with $H_3O^+(H_2O)_n$ by non dissociative proton transfer to the polymer and hence, effects current flow. Charge transfer from the ionized air to the polymer solution apparently disturbs the motion of charged species toward the collector by the formation of an ion wind. According to Fig. 3 the current developed when mineral oil was used was about the same as in the solvent-free case. This is simply because of the conductivity of mineral oil is so low—it's a non-conductive material—that

Table 2
Conductivity of the solvents

	Tap water	Methylene chloride	Acetone
Conductivity (μS)	2000	<1	<1

the mineral oil dripped from the tip of the stainless steel needle and no electrospraying occurred.

Corona discharge results in ionization of the environment. Even though solvent evaporation may increase the breakdown voltage of the gap and decrease the corona current, still, solvent molecules may undergo corona-related chemical processes. These chemical alterations may affect the outcome of the electrospinning process in terms of fiber surface modification, fiber diameter distribution, etc. It is clear that solvent evaporation and charge chemistry are major process factors in electrospinning.

3.3. Charge and mass development

The effect of deposition time on charge per mass collected on the intermediate insulated screen, or sampler, is shown in Fig. 4. The mass of fiber collected on the insulated film increased during the initial stages of electrospinning, up to perhaps 30 s. The charge per mass also decreased at perhaps a declining rate for the first minute of collection. Apparently, by about 30 s. sufficient charge has been captured by the sampler that charge repulsion steers the low inertia, charged fibers around the sampler. Simultaneously, some fibers may be losing a portion of their charge, either by neutralization by electrons or drainage. The results are consistent with Peter Tsai's measurements on electrospun webs that show electrospun fibers lose charge quickly [20].

PAN/DMF (8 wt%) solution was electrospun at two voltages: 11 and 16 kV. The lower voltage limit was chosen because fibers would not form below 11 kV in our system. The upper voltage was the highest voltage possible without inducing a significant corona discharge. The results, shown in Fig. 5, indicate that as the voltage was increased from 11 to 16 kV, the charge per mass ratio of the fibers increased. The average charge per mass increased from about 47–56 nC/mg; higher voltage, as expected, created higher charge density on the fiber.

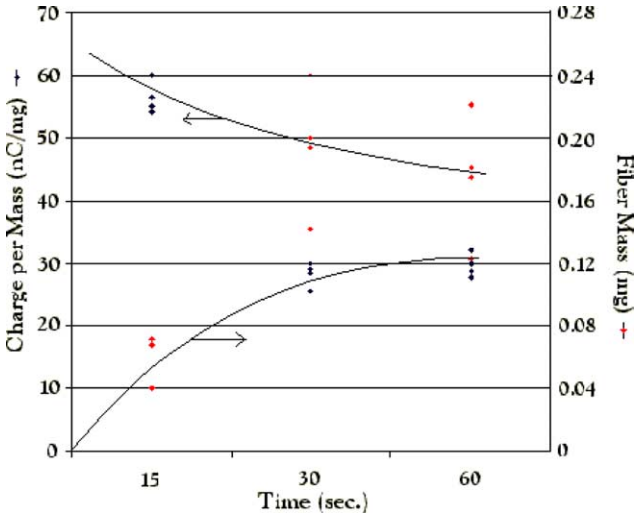

Fig. 4. Effect of fiber deposition time on the charge of electrospun PAN fibers.

Assuming that the electrical charges are mobile in the polymer solution and sufficient time is allowed for the charges to reach to the jet's surface, surface charge density can be calculated using the mass charge density and fiber diameter distribution. The calculations assume that the fibers are cylindrical, continuous and charge is uniformly distributed on the surface by the slight conductivity of the polymer. The calculation does take into account the measured (lognormal) distribution of fiber diameters. The results are given in Table 3 and show that neither the surface charge density nor the mass charge density is invariant.

3.4. Effect of solution concentration on mean fiber diameter

Two different concentrations of PAN/DMF were electrospun under constant conditions: An applied voltage of 13 kV, a feed rate of 0.005 ml/min and a needle-to-collector distance of 15.5 cm. The two solution concentrations were 8 and 13 wt%.

The results displayed graphically in Fig. 6 show that as the solution concentration increased from 8 to 13 wt%, the average charge per mass ratio decreased from 53 to 42 nC/mg, whereas the mean fiber diameter increased from 0.4 to 0.9 μm. The fiber diameter decreases with charge/mass as might have been anticipated. The fiber charge/mass ratio is not solely responsible for a fiber's diameter change. Other considerations are the viscoelastic properties of the solutions, the solvent evaporation rate, the details of the whipping motion, etc. In a recent study by Park and coworkers [21] on the electrospinning of PEO/water shows that an increase in dielectric constant of the solvent gives smaller diameter fibers and a slight addition of salt narrows the fiber diameter distributions. Fong et al. have shown the variation of beaded nanofibers arrays as net charge density changes due to the addition of NaCl [22]. The fact remains that highly viscous solutions cannot be as easily stretched as fine as a low viscosity dilute solution can be.

3.5. Negative induction charging

A representative SEM micrograph of PAN fibers electrospun using negative charging is shown in Fig. 7. The scale shown on the micrograph is 2 μm.

The diameter distribution of the negatively charged fibers was significantly narrower ($\pm$53 nm compared to $\pm$93 nm). Negatively charged fibers still follow the log normal distributions but apparently with a tighter diameter range. Since, the mass of an electron is about 10,000 times less that that of a proton, the electrons may disperse to the liquid more uniformly and more rapidly than do positive ions. Charge mobility is responsible for the conduction of the fluid and electrons move orders of magnitude faster than do even small ions. Negative induction charging yielded finer electrospun fibers than did positive charging, but the results

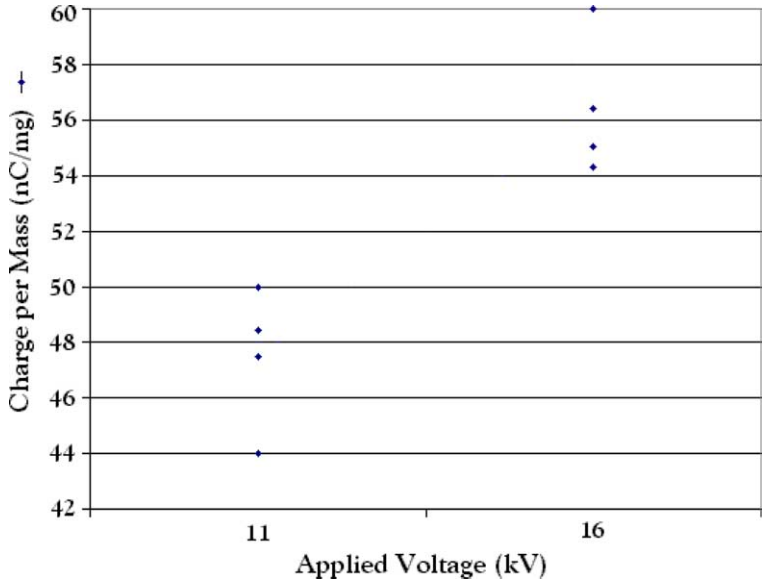

Fig. 5. Effect of applied voltage on the charge density of electrospun PAN fibers.

may not be statistically significant. The experiments need to be repeated using power supplies capable of delivering equal power. Ours operated at different power levels, the positive supply being capable of higher power as shown in Table 4.

3.6. Ionized field charging

Ionized field charging of 8 wt% PAN/DMF was also carried out. The syringe–needle system was used to pump and deliver solution. The needle and electrode were separated by 5 cm, as shown in Fig. 2. They were not in electrical contact. As the voltage applied to the ring electrode was increased, disruption of the solution at the tip of the needle was observed at a certain voltage. Ions were apparently created from neutral air molecules at atomically sharp locations, giving rise to corona formation. Since, the needle was not directly charged, it was a grounded target for the ions.

At about +30 kV, fibers were collected on the grounded electrode. A Taylor cone was not always present, but rather, spinning occurred in a pulsing mode. The conical structure of the solution at the tip of the needle would spin fibers, switch to producing droplets, and then create fibers again. This behavior was presumably a result of repeated charge accumulation in the solution, then draining by the formation of fibers when the surface charge forces exceeded surface tension.

The electrospun PAN fibers formed during ionized charging were viewed using the SEM and a representative photomicrograph is shown in Fig. 8. The scale is 2 μm, so the average fiber diameter is about 600 nm. Although in the nanometer range, the fibers are about three times larger than electrospun fibers produced using induction charging of the same solution under the same nominal conditions.

4. Theoretical calculations

Seaver [23] developed a method to calculate the surface charge density of a powder. Using his work as a basis, we derived an equation for the charge per mass of an electrospun fiber:

$$\left(\frac{q}{m_f}\right)_{max} = \frac{\varepsilon_a E_c \left(\frac{\pi d^2}{2} + \pi d h\right)}{\rho_{mf}\left(\frac{\pi d^2 h}{4}\right)} = \frac{4\varepsilon_a E_c}{\rho_{mf} d} \quad (1)$$

where q is the charge; m_f is the fiber mass; ε_a is the permittivity of free space; E_c is the electric field strength at the onset of corona; ρ_{mf} is the fiber density and d is the fiber diameter.

Table 3
Surface charge density of electrospun PAN fibers

Mass charge density (nC/mg)	Mean fiber diameter (μ)	Charge density[a] (nC/cm^2)	Charge density[b] (nC/cm^2)
42	0.9	1.05	1.1
53	0.4	0.55	0.6

[a] Surface charge density (average fiber diameter).
[b] Surface charge density (log normal fiber diameter distribution).

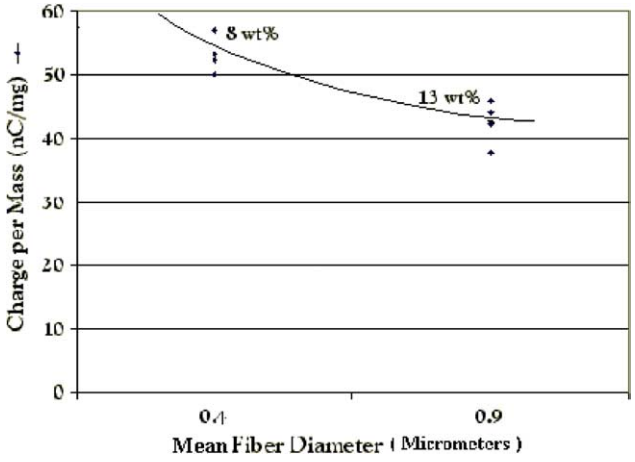

Fig. 6. Effect of solution concentration on the charge of electrospun PAN fibers.

In the paragraphs that follow we show that the theoretical values of the charge per mass obtained from this equation agree well with our experimental data; they differ by not more than a factor of 10. We also derived a charge balance model for electrospinning, and thus, calculated the charge density (charge/mass) of a given jet segment:

Before the (positive) potential is applied to a polymer solution ready for electrospinning, there are an equal number of positive and negative ions in the spinning solution. When the potential is applied, a Taylor cone and a jet form, as shown in Fig. 9, where V is the volume of the conical frustum and V_1 is the volume of space in which the jet is confined.

When the positive potential is applied to the solution, only a fraction, y, of the negative ions is neutralized due to limited contact between the solution and the charging electrode. The solution still contains $n(1-y)$ negative ions and n positive ions.

Table 4
Changes in fiber diameter by polarity and current

Polymer/solvent	Applied voltage (kV)	Current (mA)	Mean fiber diameter (nm)	Standard deviation
8 wt% PAN/DMF	−40	0.375	335	53
8 wt% PAN/DMF	+40	0.500	220	93

Two forces act on an ion moving in a viscous fluid under electric field and these are:

Electrostatic force, qE and (2)

Viscous drag force, $6\pi\eta r\mu E$ (3)

where q is the amount of charge on the ion, E is the electric field strength; η is the solution viscosity, r is the hydrodynamic radius of the ion and μ is the ion mobility.

The sum of electric field related forces is:

$$\sum F_{\text{electrostatic}} = \vec{F}_{\text{qpi}} + \vec{F}_{\text{dpi}} + \vec{F}_{\text{qni}} + \vec{F}_{\text{dni}} \tag{4}$$

where $\vec{F}_{\text{qpi}}$ is the electrostatic; and $\vec{F}_{\text{dpi}}$ is the viscous drag force acting on a positive ion; $\vec{F}_{\text{qni}}$ is the electrostatic and $\vec{F}_{\text{dni}}$ is the viscous drag force acting on a negative ion.

Inserting Eqs. (2) and (3) into Eq. (4), the sum of electrostatic forces can be expressed:

$$\begin{aligned}\sum F_{\text{electrostatic}} &= (n_1 qE) - (n_1 6\pi\eta r_{\text{pi}}\mu_{\text{pi}}E) - [n_1(1-y)qE] \\ &\quad + (n_1(1-y)6\pi\eta r_{\text{ni}}\mu_{\text{ni}}E)\end{aligned} \tag{5}$$

where n_1 is the number of ions at solution mass m; μ_{pi} and μ_{ni} are the ion mobilities of positive and negative ions.

We approximate ionic mobilities as being equal, even

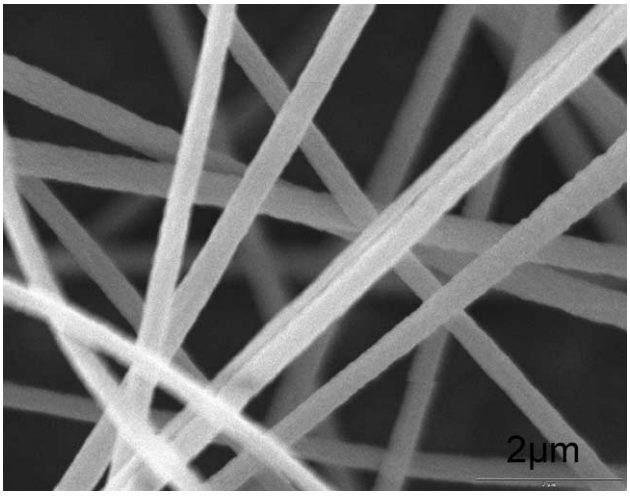

Fig. 7. SEM micrograph of electrospun PAN fibers made using −40 kV induction charging.

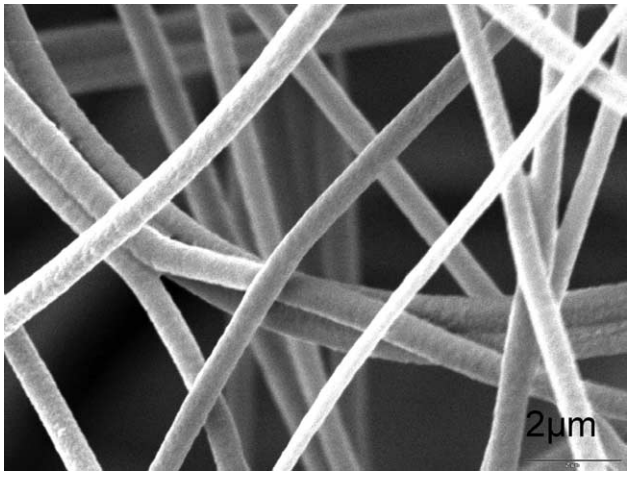

Fig. 8. SEM micrograph of electrospun PAN fibers with positive ionized field charging.

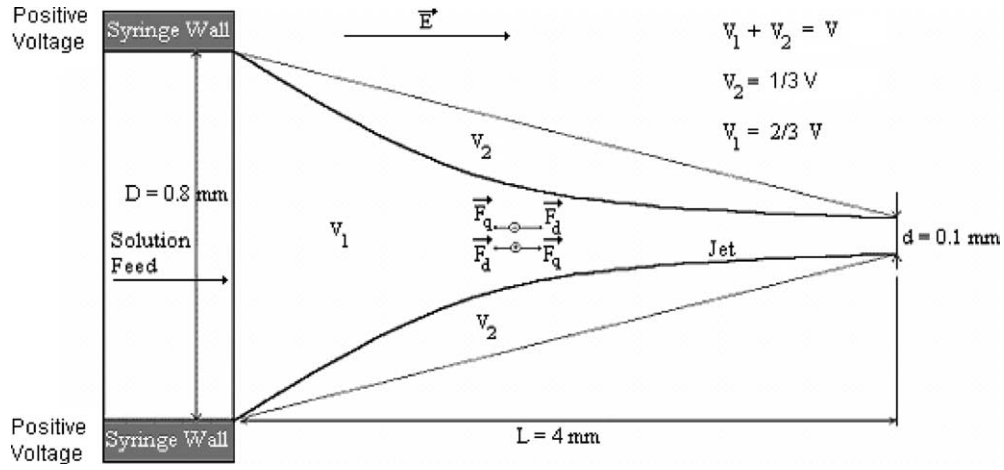

Fig. 9. Geometrical model of Taylor cone for the given jet segment.

though different ion hydrodynamic radius would result in slightly different mobilities.

Solving Eq. (5), we find:

$$\sum F_{\text{electrostatic}} = (yn_1qE) - [n_1 6\pi\eta\mu E(r_{\text{ni}} - r_{\text{pi}} - yr_{\text{ni}})] \quad (6)$$

Buer derived the forces acting on the jet [24], where the net flow of momentum is equal to the sum of forces—mechanical, gravitational, skin friction and electrostatic forces. Since, the electrostatic forces are by far the largest forces, we can establish a force balance equation (momentum conservation) taking into account only electrostatic forces. The mass and acceleration dependent part of the force balance equation is:

$$\sum F = ma = \rho\frac{2}{3}\frac{\pi h}{12}(D^2 + Dd + d^2)\frac{\mathrm{d}x^2}{\mathrm{d}t^2} \quad (7)$$

Since,

$$V = \frac{\pi h}{12}(D^2 + Dd + d^2),\ V_1 = \frac{2}{3}V,\ \text{and}\ m = \rho V_1$$

The jet volume is approximately 2/3 of the volume of a cut conical structure. This approximation was proven accurate by using a three-dimensional geometry-modeling tool. Fig. 10 shows that the software for the model has the capability to calculate individual volumes.

Setting Eqs. (6) and (7) equal gives:

$$\sum F = \rho\frac{2}{3}\frac{\pi h}{12}(D^2 + Dd + d^2)\frac{\mathrm{d}x^2}{\mathrm{d}t^2} = (yn_1qE) - [n_1 6\pi\eta\mu E(r_{\text{ni}} - r_{\text{pi}} - yr_{\text{ni}})] \quad (8)$$

The following theoretical and experimental values can be used to solve Eq. (8):

1. $\rho = 0.968$ g/cm^3, the solution density. Although solvent evaporation increases density, it is approximately constant along the jet path in the first 4 mm.
2. The diameter of the starting end of the jet was measured to be about 0.8 mm and the cut end of the jet was measured to be about 0.1 mm.
3. At $x = 0$ the velocity was measured to be 2.26 m/s and at $x = 4$ mm the velocity was measured to be 5.94 m/s [25]. The acceleration, a was calculated using these four values to be 1.7×10^5 cm/s^2.
4. y is the fraction of the negative ions neutralized by contact between the solution and the charged needle. We take it to be 10% for the sake of enabling the following calculations.
5. Negative and positive ions in the fluid are derived from impurities in the solvent. The only ions included are Cl^- and Na^+, respectively.
6. n_1 is the number of ions in a given part of the jet. Before voltage is applied (i.e. before neutralization of a portion of the negative ions) the number of positive ions equals the number of negative ions.

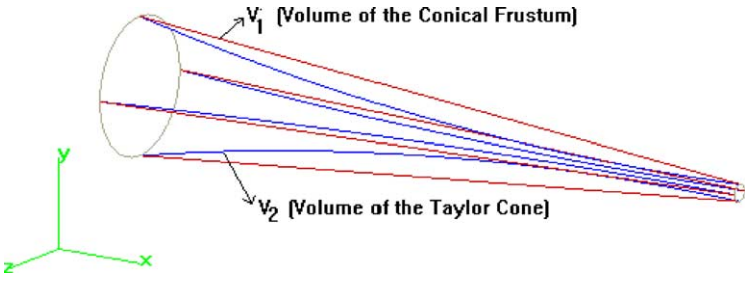

Fig. 10. Three-dimensional geometry used in volume calculations.

7. q is the elementary charge, 1.603×10^{-19} C.
8. E is the electric field strength, approximated as 1 kV/cm in the vicinity of the collection region although the field strength at the needle tip is much higher.
9. η is the measured viscosity of the 7 wt% PAN/DMF solution, 130 centipoise.
10. μ is the ion mobility. Reneker estimated it to be 1.5×10^{-7} m^2/Vs^3 for Na^+ ions under 1 kV/cm electric field strength.
11. r_{ni} and r_{pi} are the hydrodynamic radii of negative and positive ions. Since, the negative ions were approximated as Cl^-, the hydrodynamic radius is 1.69 Å. Similarly, the hydrodynamic radius of the Na^+ ions is 1.16 Å.

Eq. (8) is solved using the values above and the results show that $n_1=8.3\times10^8$; that is, there must be 8.3×10^8 ions in the first 4 mm of the jet. The calculation shows that at the start of the electrospinning process, if there are n_1 number of positive and negative ions present in the solution, then the electrostatic forces generated by these ions would be sufficient to form and accelerate a jet by transferring the momentum of the ions to the solution.

For $n_1=8.3\times10^8$, we can calculate the mass of Na^+ and Cl^- ions present in the 4 mm segment of the jet:

$$Na^+ = \frac{23\times8.3\times10^8}{6.023\times10^{23}} = 3.1\times10^{-14}\ \text{g} \tag{9}$$

$$Cl^- = \frac{35.5\times8.3\times10^8}{6.023\times10^{23}} = 4.9\times10^{-14}\ \text{g}$$

So

$$\sum Na^+Cl^- = 8\times10^{-14}\ \text{g}$$

For that segment of the jet, the solvent mass is 93% of the total mass:

$$\text{Solvent} = 0.93\times4.9\times10^{-4}\ \text{g} = 4.6\times10^{-4}\ \text{g} \tag{10}$$

Thus, the mass of the Na^+ and Cl^- ions are only a tiny fraction (less than a part per million) of the solvent mass and yet, ignoring all the other forces, electrostatic forces generated by these ions alone can cause the acceleration of the jet in the electric field direction.

Following the train of thought a bit further, the total charge in the given segment of the jet is:

$$Q = qn_{\text{total}} \tag{11}$$

$$n_{\text{total}} = n_1 + (1-y)n_1 = 1.84\times10^{11}$$

$$Q = 1.603\times10^{-19}\ \text{C}\times1.84\times10^{11} = 2.95\times10^{-8}\ \text{C}$$

$$= 29.5\ \text{nC}$$

Thus, the charge per mass (charge density) in the given jet segment is:

$$d_Q = \frac{Q}{m_j} = \frac{29.5\ \text{nC}}{4.93\times10^{-1}\ \text{mg}} = 59.8\ \text{nC/mg} \tag{12}$$

where Q is the total charge and m_j is the mass of the given jet segment.

This theoretical calculation of charge density agrees well with our experimental values. The charge density and number of ions are plotted as a function of neutralization percent (y%) of negative ions by contact charging, as shown in Fig. 11. Experimental charge density results are in close agreement with the theoretical calculations for the y value of 0.3 that seems a reasonable assumption in case of NaCl.

5. Conclusions

During electrospinning, electrical charges develop into the polymer solution (or melt), but some portion of the charge on the fiber surface may ionize the moisture in the surrounding air and thus, lose its own charge. However, solvent does not carry any charge to the surrounding while evaporating. Different experimental set-ups may give rise to more or less discharge in air; the airborne ions may interact with the fibers and the free electrons or ions may limit the solution charging. In addition, solvent evaporation is a factor in corona formation.

The charge density of electrospun fibers depends on such factors as applied voltage and solution characteristics. Charge density calculated from theory is in good agreement with the experimental values.

The polarity of induction charging does not play a significant role in nanofiber formation, suggesting that the enhanced mobility of the charge carriers is not significant in the processes of fiber formation. Fiber diameters of a hundred nanometers or less can be achieved using either positive or negative charging. Properties of electrospun fibers created using negative induction charging should be investigated further and compared to those of fibers made using positive induction charging.

Electrospinning of polymer solution can be achieved not only using induction charging but also by using ionized field charging. Although it may not be a promising method of fiber production, it proves that discharge into the air can be manipulative. The fiber diameters were about three times higher than those of fibers produced by induction charging under the same conditions.

Acknowledgements

The authors would like to thank the National Textile Center for funding Project M01-D22; Prof McCarthy of Polymer Science and Engineering, UMass, Amherst, for his

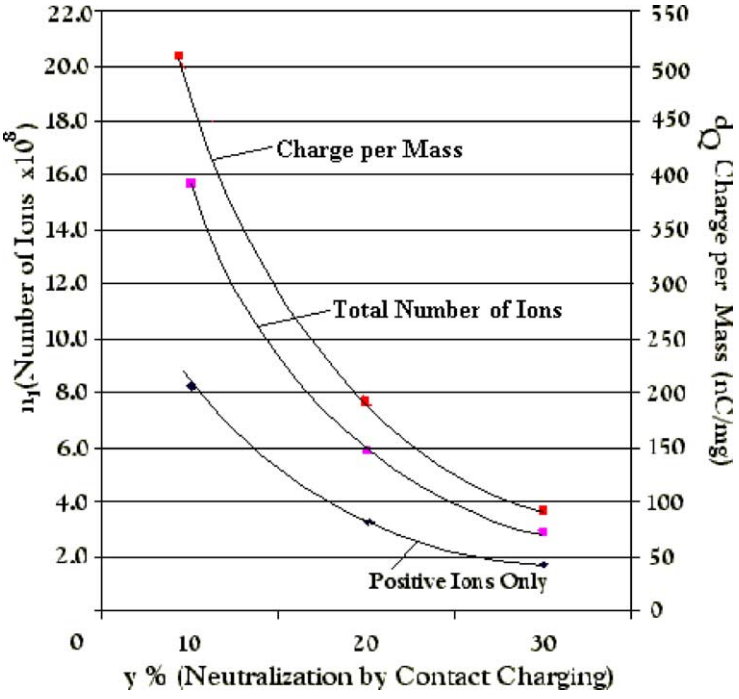

Fig. 11. Charge density and number of ions as a function of neutralization percentage.

help in contact angle measurements; and Mr Leo Barish for his assistance with and discussions regarding the SEM studies.

References

[1] Buer A, Ugbolue SC, Warner SB. Textile Res J 2001;71(4):323.
[2] Tan EPS, Ng SY, Lim CT. Biomaterials 2005;26:1453.
[3] Reneker DH, Yarin AL, Fong H, Koombhongse S. J Appl Phys 2000; 87:1.
[4] Jin HJ, Fridrikh SV, Rutledge GC, Kaplan DL. Biomacromolecules 2002;3:123.
[5] Dzenis Y. Science 2004;304:1917.
[6] Hagewood J. Joint, INDA-TAPPI Conference. Baltimore: MD; 2003 16–18.
[7] Warner SB, Perkins CA, Abhiraman AS. INDA J Nonwovens Res 1995;2:33.
[8] Wilson J. In: Nonwoven World, August–September; 2001.
[9] Taylor GI. Proc R Soc London, Ser A 1969;313:453.
[10] Shortkroff S, Li Y, Thornhill TS, Rutledge GC. Polym Mater Sci Eng 2002;87:457.
[11] Gibson P, Gibson HS. In: 10th Annual International TANDEC Nonwovens Conference; 2000.
[12] Wang M, Singh H, Hatton TA, Rutledge GC. Polymer 2004;45:5505.
[13] Law SE, Bowen HD. Trans ASAE 1966;501.
[14] Gaskell SJ. J Mass Spectrom 1997;32:677.
[15] Kelly AJ. J Aerosol Sci 1994;25:1159.
[16] Kessick R, Fenn J, Tepper G. Polymer 2004;45:2981.
[17] Dono A, Paradisi C, Scorrana G. Rapid Commun Mass Spectrom 1997;11:1687.
[18] Kucerovsky Z, Greason WD, Ieta A. J Electrostat 2001;50:147.
[19] Allen KR, Phillips K. Nature 1959;183:174.
[20] Tsai P, Gibson SH, Gibson P. J Electrostat 2002;54(3/4):333.
[21] Son WK, Youk JH, Lee TS, Park WH. Polymer 2004;45:2959.
[22] Fong H, Chun I, Reneker DH. Polymer 1999;40:4585.
[23] Seaver AE. In: Proceedings ESA Annual Meeting 1999; 29.
[24] Buer A, MSc Textile Technology Thesis. University of Massachusetts: Dartmouth; 2000.
[25] Reneker DH, Chun I. Nanotechnology 1996;7:216.